Supplementary information

Maternal exposure to polystyrene nanoplastics causes brain abnormalities in progeny

Bohyeon Jeong[1,2], Young-Kyoung Ryu[3], Jeong Yeob Baek[1], Jahong Koo[1,2], Subin Park[1], Seungjae Zhang[4], ChiHye Chung[4], Rumeysa Dogan[5], Hyung-Seok Choi[5], Dahun Um[5], Tae-Kyung Kim[5], Wang Sik Lee[6], Kyoung-Shim Kim[3], Jinyoung Jeong[6], Won-Ho Shin[7], Jae-Ran Lee[1], Nam-Soon Kim[1], and Da Yong Lee[1,2]*

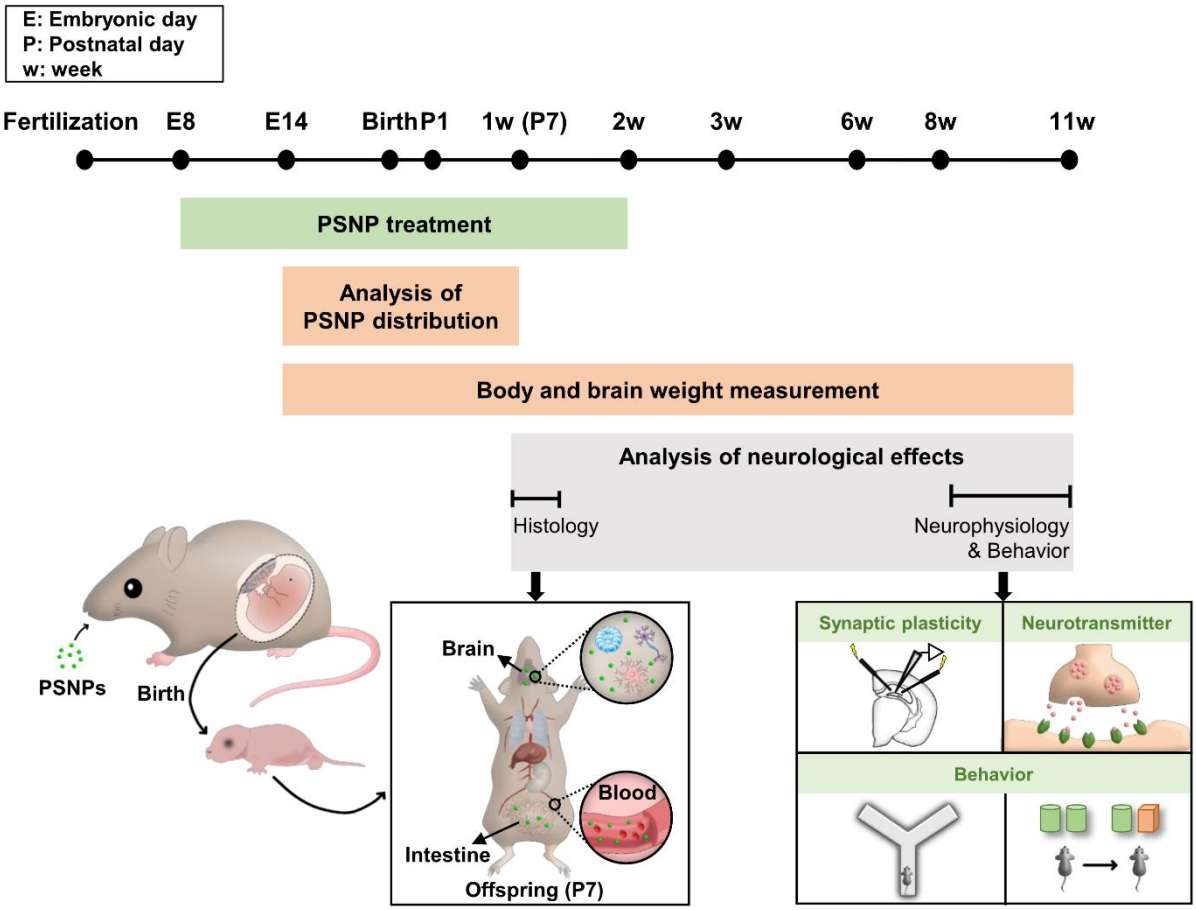

Supplementary Fig 1. Schematic drawing showing the overall experimental procedure and time schedules for PSNP treatment and physiological analyses.

Supplementary Table 1. Summary of the protocols used to administer PSNPs to rodents.

Species	Study	Diameter	Administration		Dose
Mice	Morh et al., 2014[1]	100 nm	Single injection Sacrificed at day 4	IV injection	0.37 μg
	Deng et al., 2017[2]	5–20 μm	Daily For 28 days	Oral gavage	0.1 mg/day
	Lu et al., 2018[3]	0.5–50 μm	Continuous For 5 weeks	Diluted in drinking water	100–1,000 μg/L
	Stock et al., 2019[4]	1–10 μm	Three times a week For 28 days	Oral gavage	1.25–34 mg/kg
	Jin et al., 2019[5]	5 μm	Continuous For 6 weeks	Diluted in drinking water	100–1,000 μg/L
	Jin et al., 2021[6]	0.5–10 μm	Daily For 28 days	Oral gavage	1 mg/day
Rats	Jani et al., 1989[7]	100 nm–3 μm	Daily For 10 days	Oral gavage	1.25 mg/kg
	Hillery et al., 1996[8]	60 nm	Daily For 5 days	Oral gavage	14 mg/kg
	Rafiee et al., 2018[9]	25–50 nm	Daily For 35 days	Oral gavage	1–10 mg/kg/day

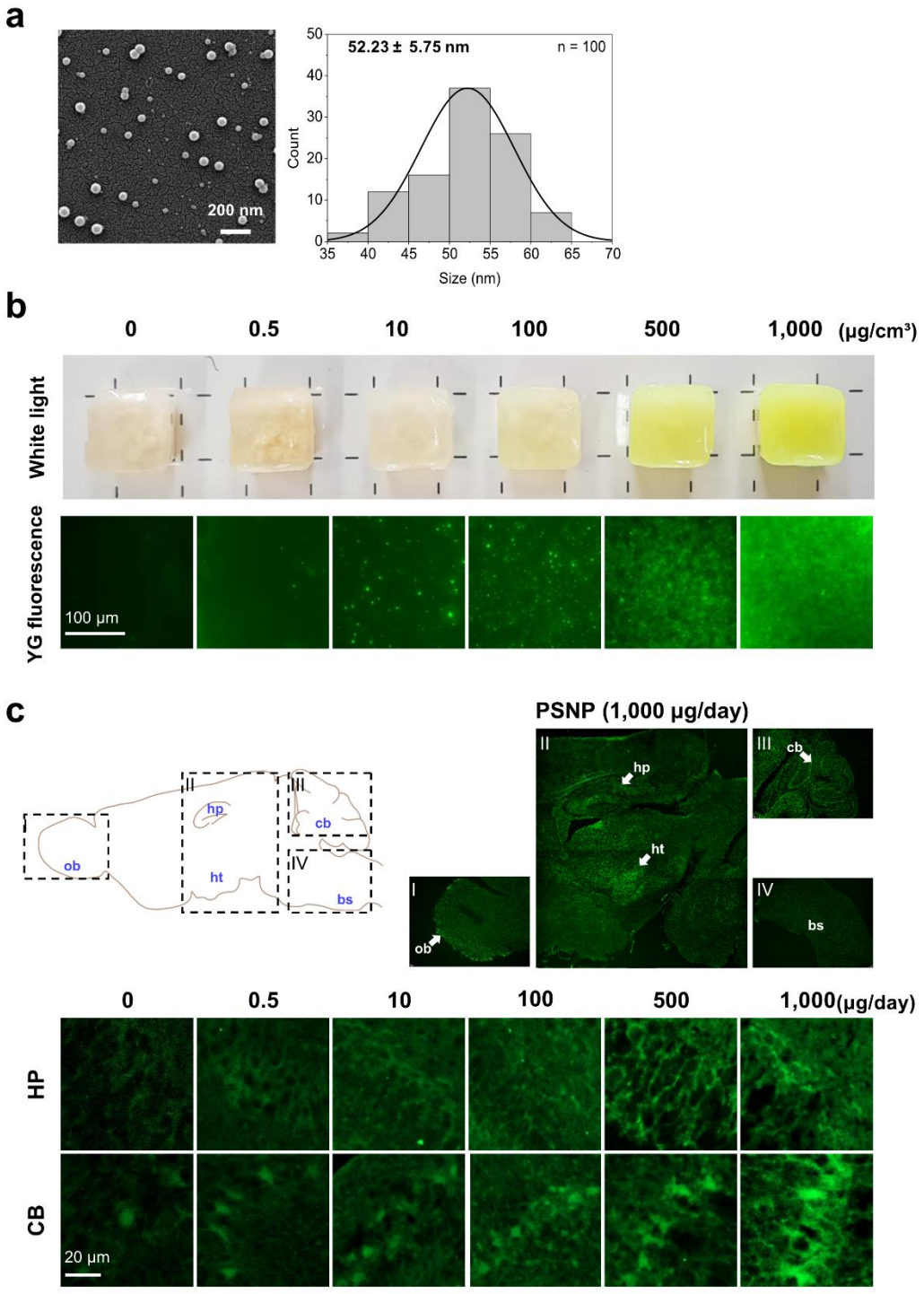
a
200 nm
52.23 ± 5.75 nm
n = 100
Count
Size (nm)
b
0
0.5
10
100
500
1,000 (μg/cm³)
White light
YG fluorescence
100 μm
c
PSNP (1,000 μg/day)
ob
hp
ht
cb
bs
0
0.5
10
100
500
1,000(μg/day)
HP
CB
20 μm

Supplementary Fig 2. Maternally-administered PSNPs accumulated in the brains of offspring. (**a**) The size distribution of the 50 nm carboxylated PSNPs was confirmed by SEM imaging. (**b**) White light images show the appearance of jelly cubes containing PSNPs (0–1,000 μg/cm^3 cube). The YG fluorescence images show higher green fluorescence signal with higher concentrations of YG-conjugated PSNPs in the jelly cubes. (**c**) YG fluorescence signals were detected in various regions of the brain including olfactory bulb (ob), hippocampus (hp), hypothalamus (ht), and cerebellum (cb), but not in brainstem (bs) in the brain sagittal view of the PSNP treated group (P7; 1,000 μg/day). Fluorescence images show higher signal intensity in the postnatal brains of the progeny given higher PSNP doses.

Supplementary Table 2. The effects of PSNPs at various doses and time points on the body weights of progeny.

Time / (μg/day)	1w			3w			6w			11w		
	n	Mean	SEM	n	Mean	SEM	n	Mean	SEM	n	Mean	SEM
0	38	3.57	0.07	29	8.50	0.27	24	17.69	0.46	17	23.54	0.81
0.5	19	3.43	0.07	15	8.31	0.30	15	*19.37	0.65	15	23.36	0.85
10	14	3.80	0.12	10	9.24	0.22	10	19.26	0.51	10	22.09	0.65
100	9	*3.93	0.08	7	8.59	0.27	7	**20.53	0.68	7	23.89	0.74
500	44	†††***4.07	0.07	28	*9.22	0.18	26	††**20.17	0.51	16	24.20	0.93

$^{*}p < 0.05$, $^{**}p < 0.005$ by t-test; $^{\dagger\dagger}p < 0.005$, $^{\dagger\dagger\dagger}p < 0.0005$ by ANOVA test

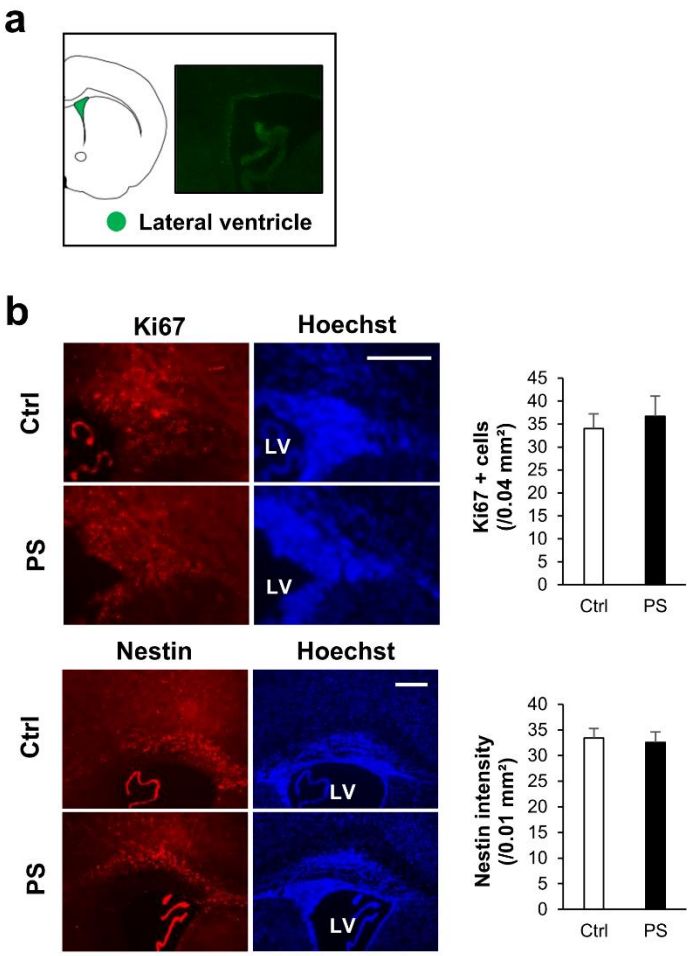

37

38 **Supplementary Fig 3. The proliferation of NSCs in the subventricular zone (SVZ) was not altered**
39 **by PSNPs.** (**a**) No YG fluorescence signal was detected in the SVZ after PSNP exposure. (**b**)
40 Immunofluorescence staining data shows no change in Ki67+ or nestin+ progenitor cells in the SVZ
41 after PSNP treatment. Values denote mean ± SEM. Scale bars: 200 μm.

42

43

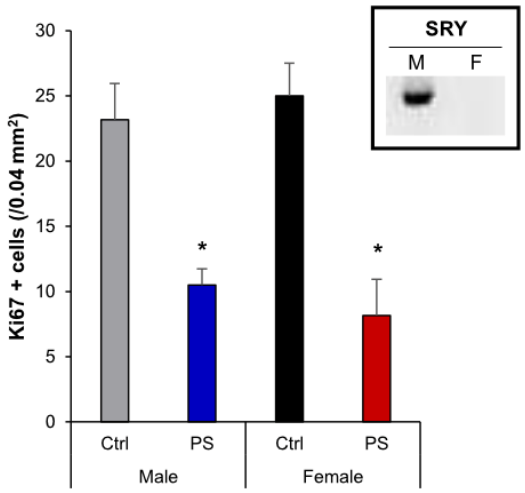

Supplementary Fig 4. PSNP reduced NSC proliferation in the brains of postnatal progeny regardless of their gender. The gender of the mouse pups used in the hippocampal Ki67 immunohistochemistry presented in **Fig 3a** was confirmed by genotyping with SRY primer (*see inset*). No correlation between the mouse gender and the number of Ki67+ cells was observed in P7 mouse brain after PSNP (500 μg/day) treatment. Values denote mean ± SEM. *$p < 0.05$.

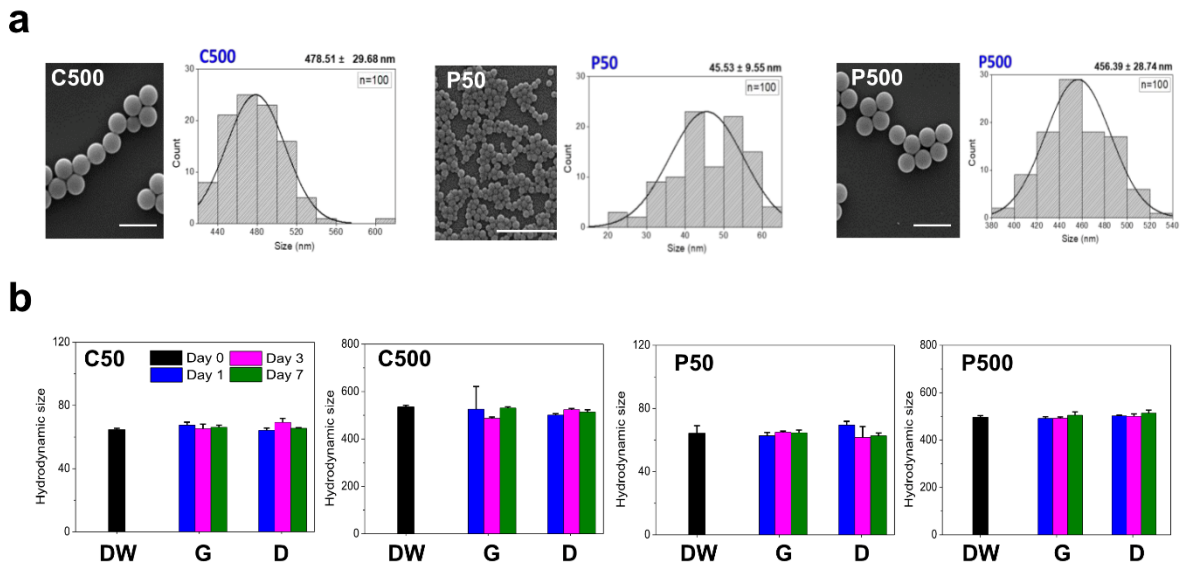

	DW	C50	C500	P50	P500
	R_H (nm)	64.70 ± 0.85 nm	535.0 ± 7.17 nm	64.30 ± 4.77 nm	496.2 ± 6.92 nm
Growth	NSC w/ growth factors	C50	C500	P50	P500
	Day 1	67.53 ± 1.89 nm	525.43 ± 95.98 nm	62.73 ± 2.04 nm	491.27 ± 7.06 nm
	Day 3	65.27 ± 2.89 nm	486.80 ± 5.86 nm	64.93 ± 0.76 nm	492.17 ± 5.35 nm
	Day 7	66.23 ± 1.29 nm	530.67 ± 5.16 nm	64.60 ± 1.71 nm	504.73 ± 13.95 nm
Differentiation	NSC w/o growth factors	C50	C500	P50	P500
	Day 1	64.23 ± 1.46 nm	500.80 ± 6.09 nm	69.47 ± 2.38 nm	502.17 ± 3.10 nm
	Day 3	69.30 ± 2.51 nm	523.73 ± 5.17 nm	61.57 ± 6.96 nm	500.00 ± 10.27 nm
	Day 7	65.53 ± 0.40 nm	513.13 ± 9.91 nm	62.63 ± 1.80 nm	513.70 ± 12.74 nm

Supplementary Fig 5. SEM images and DLS analysis data show that all four types of PSNPs were stably maintained as separate particles in culture conditions. (**a**) Carboxylated and plain spheroid PSNPs with two different diameters (50 and 500 nm) were characterized by SEM imaging. (**b**) DLS analysis data show that all four types of PSNP particles were well maintained for 7 days in DW and culture media for both growth and differentiation. Scale bars: 1 μm. C: carboxylated PSNP; P: plain PSNP; 50: 50 nm; 500: 500 nm

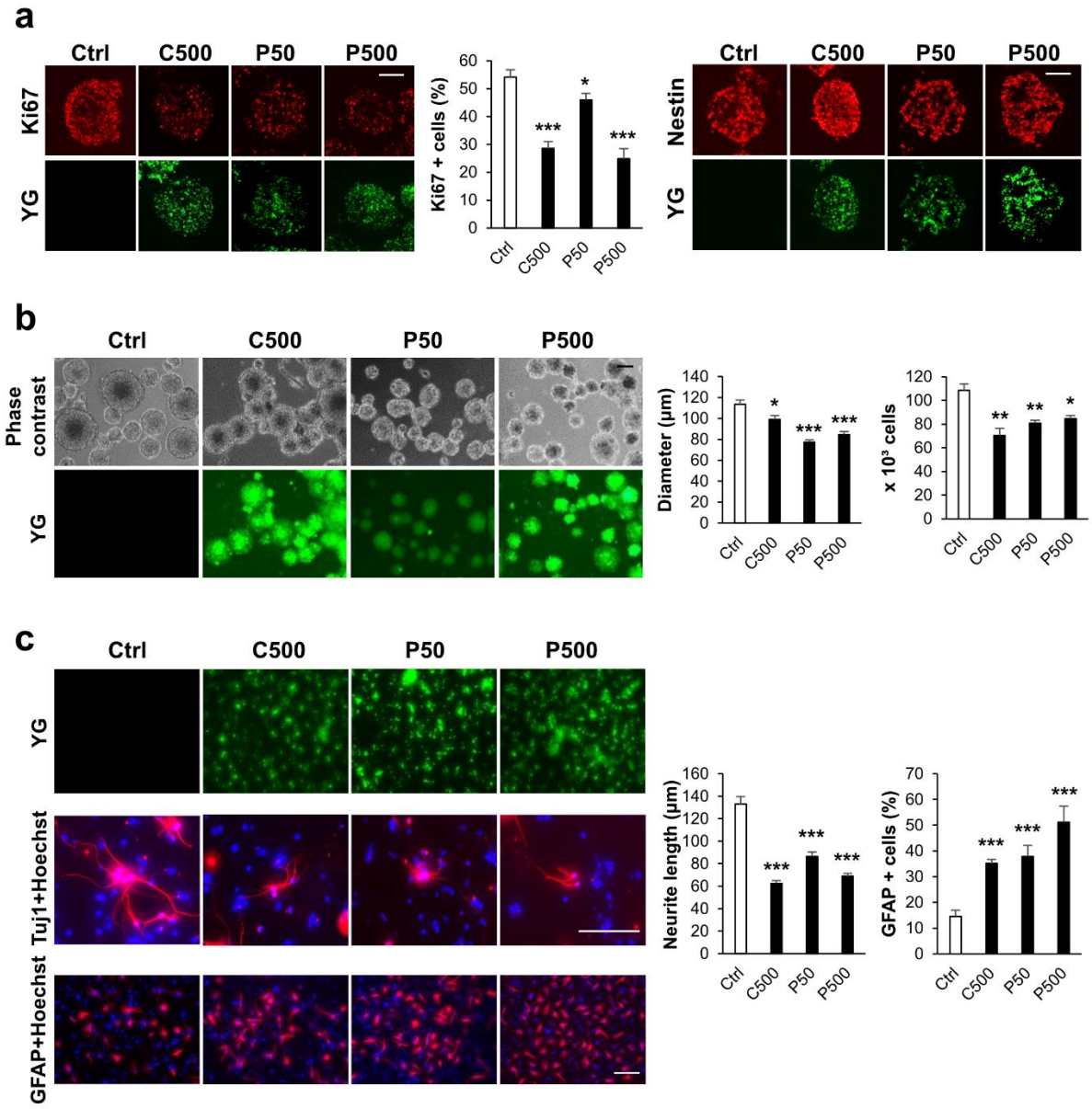
a
Ctrl
C500
P50
P500
Ki67
YG
Ki67 + cells (%)
Nestin
b
Phase contrast
Diameter (µm)
x 10³ cells
c
Tuj1+Hoechst
GFAP+Hoechst
Neurite length (µm)
GFAP + cells (%)

Supplementary Fig 6. The functioning of NSCs in vitro was altered by various types of PSNPs. (**a**) Immunofluorescence staining of single neurospheres shows lower Ki67+ proliferative NSCs following exposure to all three different types of PSNPs (25 μg/ml). Other staining data show that nestin was well expressed in the neurospheres of all four groups, including the control and three PSNP-exposed groups. YG fluorescence signals (green) were detected in all PSNP-exposed groups. (**b**) Smaller neurosphere diameters and lower total cell numbers were observed in all three PSNP-exposed groups in comparison with the controls (Ctrl). (**c**) NSC differentiation assay data show a shorter neurite length of Tuj1+ neurons and a higher number of GFAP+ astrocytes in 25 μg/ml PSNP-treated groups than in controls. Values denote mean ± SEM. *$p < 0.05$, **$p < 0.005$, ***$p < 0.0005$. Scale bars: 100 μm. C: carboxylated PSNP; P: plain PSNP; 50: 50 nm; 500: 500 nm.

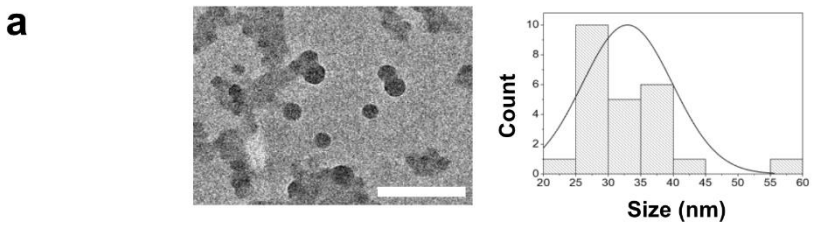

Diameters	Hydrodynamic size (DLS, nm)	SEM analysis (Average size, nm)
30 nm	41.07 ± 3.74 nm	32.95 ± 6.95 nm

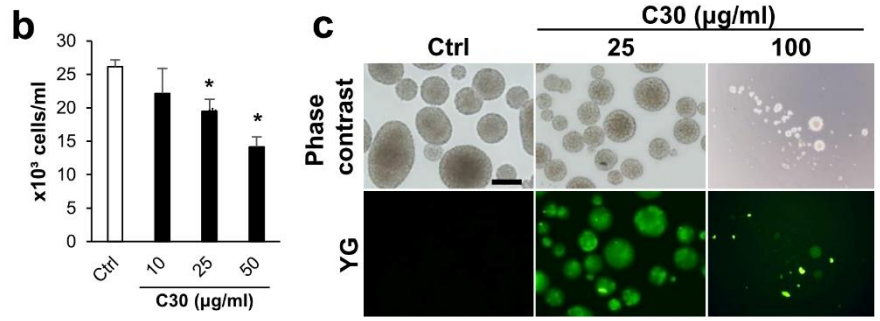

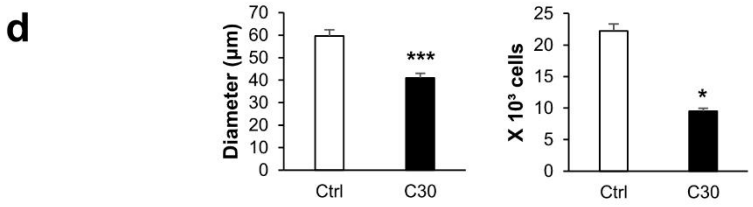

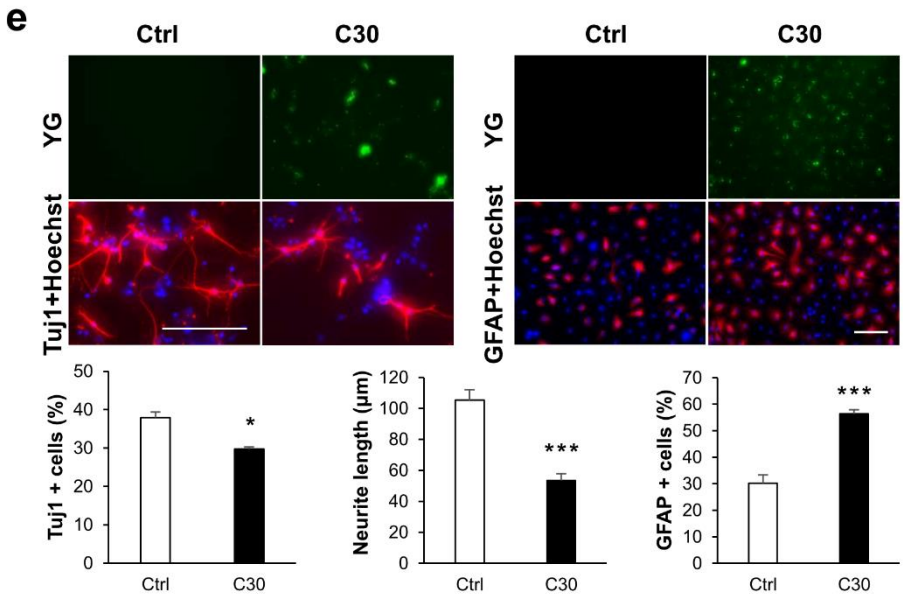

Supplementary Fig 7. Carboxylated PSNPs of 30 nm in diameter dysregulated NSC functions in a similar manner to other types of PSNPs. (**a**) Carboxylated PSNPs (C30) were characterized by TEM imaging and DLS analysis. (**b**) Exposure to C30 reduced the proliferation of NSCs in a dose-dependent manner. (**c**) Phase contrast images show smaller neurosphere sizes following C30 exposure (25 μg/ml). The highest concentration of C30 (100 μg/ml) induced severe cytotoxicity. (**d**) The diameters of neurospheres and total cell numbers were lower after exposure to C30 (25 μg/ml). (**e**) Differentiation assay data show lower numbers of neurons, shorter neurite lengths, and abnormally high levels of astrocytes in the C30-exposed group. YG fluorescence signals (green) were detected in all C30-exposed groups. Values denote mean ± SEM. *$p < 0.05$, ***$p < 0.0005$. Scale bars: (**a**) 200 nm, (**c, e**) 100 μm.

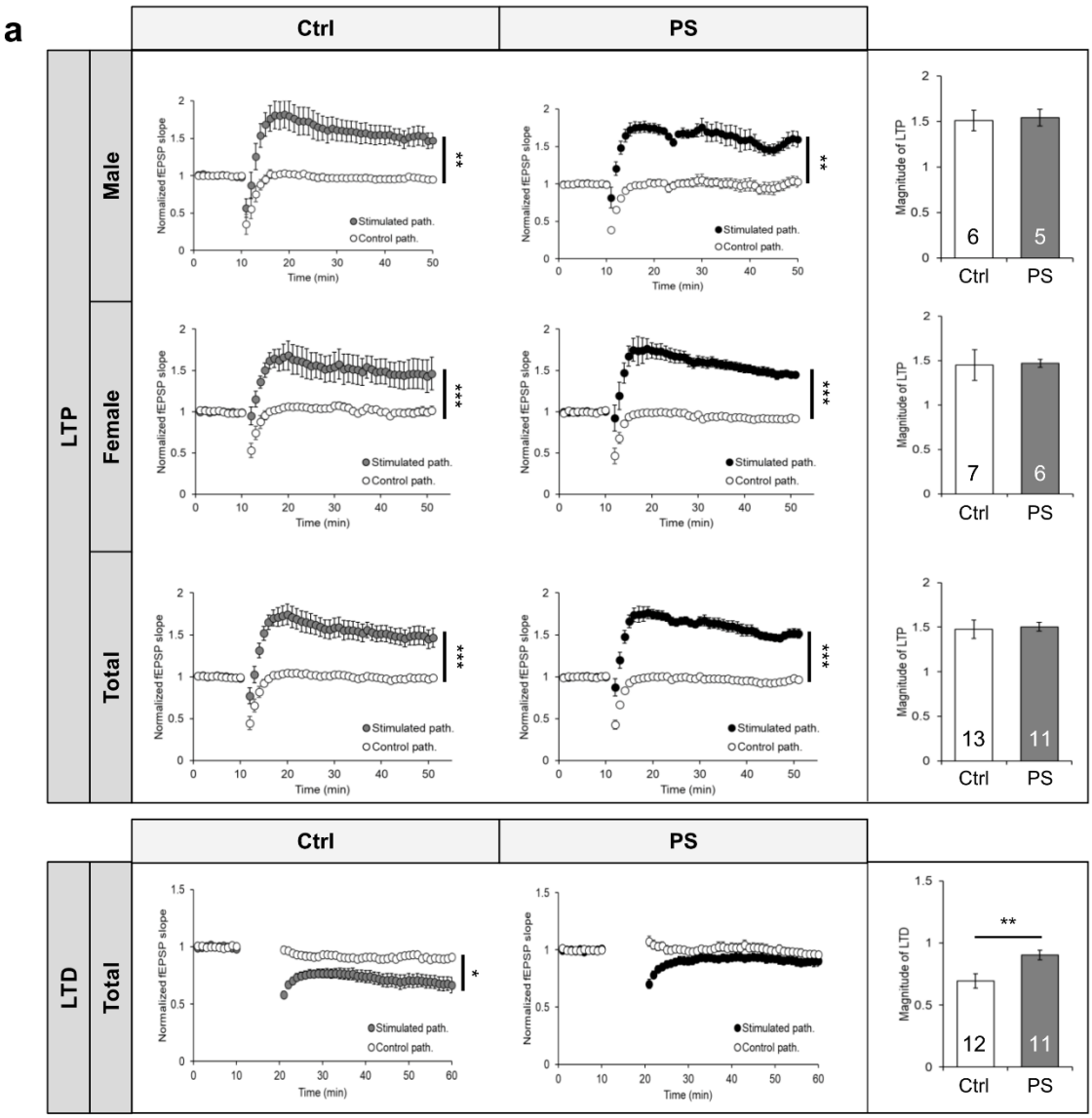
a
Ctrl
PS
LTP
Male
Female
Total
Normalized fEPSP slope
Time (min)
Stimulated path.
Control path.
**
***
Magnitude of LTP
6
5
7
6
13
11
Ctrl
PS
LTD
Total
*
Magnitude of LTD
12
11
b
Hippocampus
Cortex
Glutamate (μg/mg)
GABA (μg/mg)
Ctrl
PS

85

Supplementary Fig 8. Carboxylated PSNPs of 50 nm in diameter caused abnormalities in synaptic plasticity and hippocampal GABA levels. (**a**) Four episodes of theta burst stimulation (4×TBS) successfully increased the rise slope of field excitatory postsynaptic potentials (fEPSPs) in both control and PSNP-exposed mice, whereas LFS decreased the rise slope of fEPSPs in the control group but not in the PSNP-exposed group. (**b**) The HPLC results show higher GABA levels in the hippocampus of progeny exposed to PSNPs. Values denote mean ± SEM. *$p < 0.05$, **$p < 0.01$, ***$p < 0.001$.

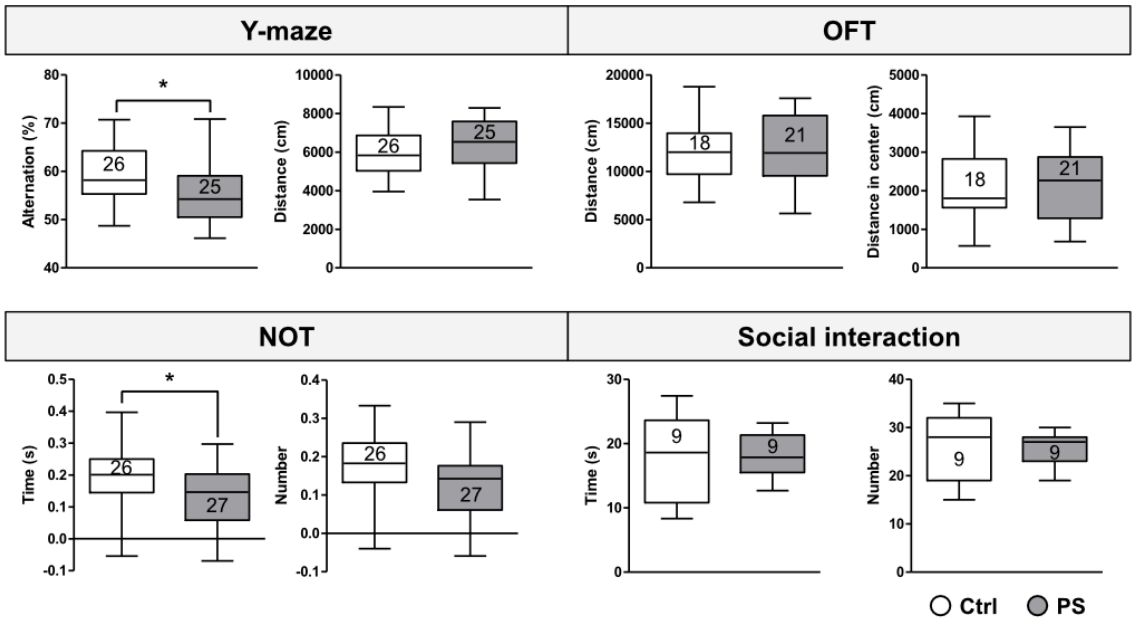

94

95 **Supplementary Fig 9. Carboxylated PSNPs of 50 nm in diameter caused cognitive deficit.** The
96 graphs show lower Y-maze alternation and NOT exploration time in the progeny exposed to PSNPs,
97 indicating that they showed cognitive deficit. Values denote mean ± SEM. *$p < 0.05$.

98

Supplementary materials and methods

Electron microscopy

The C30 particles were characterized by TEM imaging. PSNPs (50, 500 nm) used in this study were characterized by scanning electron microscope (SEM) imaging[10].

Dynamic light scattering (DLS) analysis

Dynamic light scattering (DLS) analysis was performed as previously described[10]. To confirm the stability of NPs in the culture media used in the current study, the NPs were subjected to DLS analysis in the condition equivalent to NSC cultures in vitro at day 1, 3 and 7.

Sex genotyping of P7 mice

Total DNA was extracted from the brain tissues using an Exgene Tissue SV mini kit (GeneAll, Korea). SRY primers were used for genotyping to determine the gender of the P7 mice. The primer sequences were as follows: forward 5'-TTG TCT AGA GAG CAT GGA GGG CCA TGT CAA-3' and reverse 5'-CCA CTC TGT GAC ACT TTA GCC CTC CGA[11].

Yellow-Green fluorescence-labeled 30 nm carboxylated PSNPs

Yellow-Green fluorescence (YG)-labeled 30 nm carboxylated PSNPs (C30) were purchased from MilliporeSigma (Cat# L5155; St. Louis, MO). These PSNPs (2.5% w/v aqueous suspensions) have a negatively charged carboxyl (COOH-) group and YG conjugated to their surface.

Supplementary references

1 Morh, K. *et al.* Aggregation behavior of polystyrene-nanoparticles in human blood serum and its impact on the *in vivo* distribution in mice. *J Nanomed Nanotechnol.* **5**, 193 (2014).

2 Deng, Y., Zhang, Y., Lemos, B. & Ren, H. Tissue accumulation of microplastics in mice and biomarker responses suggest widespread health risks of exposure. *Scientific reports* **7**, 46687 (2017).

3 Lu, L. *et al.* Polystyrene microplastics induce gut microbiota dysbiosis and hepatic lipid metabolism disorder in mice. *Sci. Total Environ.* **631-632**, 449-458 (2018).

4 Stock, V. *et al.* Uptake and effects of orally ingested polystyrene microplastic particles in vitro and in vivo. *Arch Toxicol.* **93(7)**, 1817-1833 (2019).

5 Jin, Y. *et al.* Impacts of polystyrene microplastic on the gut barrier, microbiota and metabolism of mice. *Sci. Total Environ.* **649**, 308-317 (2019).

6 Jin, H. *et al.* Polystyrene microplastics induced male reproductive toxicity in mice. *J. Hazard. Mater.* **401**, 123430 (2021).

7 Jani, G. W. *et al.* The uptake and translocation of latex nanospheres and microspheres after oral administration to rats. *J Pharm Pharmacol.* **41**, 809-812 (1989).

8 Hillery, A. M. *et al.* The effect of adsorbed poloxamer 188 and 407 surfactants on the intestinal uptake of 60-nm polystyrene particles after oral administration in the rats. *Int. J. Pharm.* **132**, 123-130 (1996).

9 Rafiee, M. *et al.* Neurobehavioral essessment of rats exposed to pristine polystyrene nanoplastics upon oral exposure. *Chemosphere* **193**, 745-753 (2018).

10 Lee, W. S. *et al.* Bioaccumulation of polystyrene nanoplastics and their effect on the toxicity of Au ions in zebrafish embryos. *Nanoscale* **11**, 3173-3185 (2019).

11 Park, S. E. *et al.* Contribution of zinc-dependent delayed calcium influx via TRPC5 in oxidative neuronal death and its prevention by novel TRPC antagonist. *Mol Neurobiol* **56**, 2822-2835 (2019).